Molecular-Beam Scattering Experiments and Theoretical Calculations Probing Charge Transfer in Weakly Bound Complexes of Water†

L. F. Roncaratti,‡ L. Belpassi,§ D. Cappelletti,|| F. Pirani,‡ and F. Tarantelli*,§

Dipartimento di Chimica, Università di Perugia, 06123 Perugia, Italy, Dipartimento di Chimica, Università di Perugia, and CNR I.S.T.M, 06123 Perugia, Italy, and Dipartimento di Ingegneria Civile e Ambientale, Università di Perugia, 06125 Perugia, Italy

Received: June 15, 2009

We describe and analyze in depth a series of molecular beam scattering experiments, first reported by Aquilanti et al. (*Angew. Chemie Int. Ed.* **2005**, *44*, 2356.), proving that a measurable bond stabilization component beyond the van-der-Waals forces is present in the prototypal hydrophobic interaction of water with the noble gases (Ng). The experimental integral cross-section data, exhibiting a fully resolved "glory" interference pattern in the velocity dependence, are here quantitatively analyzed and characterized employing a recently proposed model potential. The stabilization component of the water−Ng bond has recently been attributed, through very accurate theoretical calculations and an unambiguous, model-free analysis of the electron density displacement, to a net electron transfer taking place from Ng to H_2O. We review the theoretical analysis and discuss additional computational results, comparing them to experiment, that clarify the effect of charge transfer on the interaction energies.

Introduction

Complexes between water and other closed shell species bind through noncovalent hydrophobic and hydrophilic interactions[1] and are of importance in both gaseous and condensed phases. Among such noncovalent interactions the most characteristic is the hydrogen-bond (H-bond). Because of its outstanding relevance for the description of water properties (the ice phase, the liquid state including its role as a solvent, the water dimer and higher order clusters,...) the H-bond has been persistently the target of experimental and theoretical investigations, addressed at understanding its manifestation and peculiar features.[2]

In recent years many new topics have been added to this broad research area.[3] In particular, many researchers focused their attention on the mechanism of electronic reorganization in weakly bound complexes, which leads to conventional or to improper H-bonding (see for instance ref 4). The possible charge-transfer nature of an H-bond is one of the more interesting but also controversial issues (even if not really new, see for example, ref 5) and has recently strongly come back to attention because of experiments interpreted as direct evidence of a partial covalency of some H-bonded systems.[6] Indeed, a detailed description of the nature of the H-bond, would require us to account for the critical balancing of electrostatic, charge transfer (CT), induction, dispersion, and exchange (or size) repulsion components of the interaction, and this subject continues today to present many open questions.[7] Several well-established energy and charge decomposition schemes available from quantum chemistry[8−11] may be usefully brought to bear on this problem, although, especially in the case of very weak interactions, the energy terms involved are exceedingly small (a fraction of kJ/mol) and may be elusive to both calculations and experiments.

Another interest arises from the evidence that weakly interacting complexes of water in the gas phase lead to collisional complexes, either stable or metastable, that can play relevant roles in atmospheric chemistry and physics.[12] In particular, complexes involving water and air components have been suggested as possible contributors to the absorption of solar radiation[13] in the infrared region, thus affecting the energy balance of the Earth atmosphere. The detailed characterization of dynamical and optical properties of these weakly interacting species is still unsatisfactory[14] and requires the knowledge of more reliable potential energy surfaces. In this respect, the modeling of various components of the overall noncovalent interaction is an issue of general and great interest.[15] Over the years we have dedicated much effort to the understanding of how the features of the interaction change as different systems are considered: the modeling of the diverse components in terms of monomer properties requires appropriate combinations and extensions of experimental and theoretical information on prototypal aggregates.[16,17]

Systems involving closed shell molecules interacting with other nonpolar closed shell particles generally bind through the well-known van-der-Waals (vdW) interaction, which we define here as due to the combination of short-range size repulsion with long-range dispersion attraction (note that different definitions may be available in the literature), to which a small induction effect often adds, as in the case of the water molecule. In this paper we focus on the simplest water aggregates, those with the five noble gases (Ng). For them, contributions to the interaction from the electrostatic component are absent,[15] and the remaining ones are hopefully amenable to proper testing and modeling: the question is whether the simple vdW picture suffices, or whether there is more to it. Previous experimental and theoretical studies were mostly focused on H_2O−He[18−20] and H_2O−Ar.[21−23] In particular, Cohen and Saykally[21] obtained a very accurate potential energy surface (AW2) for H_2O−Ar

† Part of the "Vincenzo Aquilanti Festschrift".

* Corresponding author. E-mail: franc@thch.unipg.it.
‡ Dipartimento di Chimica, Università di Perugia, 06123 Perugia, Italy.
§ Dipartimento di Chimica, Università di Perugia, and CNR I.S.T.M, 06123 Perugia, Italy.
|| Dipartimento di Ingegneria Civile e Ambientale, Università di Perugia, 06125 Perugia, Italy.

10.1021/jp905584p
Published on Web 08/25/2009

from the analysis of absorption measurements carried out in various spectral regions. Information on the molecular structure of the H_2O-Kr and H_2O-Xe systems was also obtained from microwave spectroscopy.[24,25] However, a systematic and internally consistent study of the strength of the interaction involved and of its variation along the entire Ng series is lacking. This was the main motivation of the present work.

It is well-known[26] that experimental information on the absolute scale of weak intermolecular interactions in the potential well region can be accurately provided only by second virial coefficient values, especially when measured in a wide interval including the low-temperature range, and by cross section data measured under high resolution conditions. For some water−Ng systems second virial coefficients have been obtained from measurements of the solubility of ice in a noble gas. However, such data, available with a large uncertainty and in a narrow temperature range, provide limited information on the intermolecular interaction.[18,23]

In 2005 we performed a series of experiments using a velocity selected water molecular beam (MB) scattered by He, Ne, Ar, Kr, and Xe gaseous targets to measure the integral cross section Q and its dependence from the MB velocity v. A preliminary analysis of these experiments, together with some quantum chemical calculations, were then reported.[27] If only vdW interactions were at work, O_2 and water would be expected to interact comparably with the same Ng atom, and thus to show a very similar $Q(v)$ function. This indeed was found to be the case for the complexes with He and Ne. However, we observed a marked difference in the measured $Q(v)$ of O_2 and water when scattered by the heavier Ngs. In particular, the systems involving water exhibit a shift of the "glory" extrema position toward higher collision velocities. This shift, increasing along the Ng series, was tentatively associated with an additional stabilizing interaction component emerging at short-range in the systems involving water.[27] However, a conclusive and satisfactory explanation of the observed effects remained unavailable. In a recent communication,[28] which also summarized the results of additional experiments confirming those findings, we have conclusively shown, through accurate ab initio calculations, that the bond stabilization in the water complexes is directly and quantitatively related to a net electron transfer from the noble gas to H_2O. In the present paper we give a complete and detailed description of the molecular beam scattering experiments revealing the bond stabilization in the water complexes. For their analysis we employ a recently proposed, improved, model potential[29] for the interaction. We also briefly review the theoretical electron density analysis that led us to ascertain the presence of a CT component in the interaction and we discuss in detail additional aspects and results of the calculations, comparing them with the experiments.

Scattering Experiments

The experiments are carried out in a MB apparatus that operates under high angular and velocity resolution conditions, providing the integral cross section Q as a function of collision velocity v in a range were modulations due to quantum interference (the "glory" effect) is exhibited. Such observables are very sensitive to the features of the interaction between projectile and target. The MB contains rotationally "hot" water molecules, whose scattering by a Ng is basically driven by the rotationally averaged (isotropic) component of the interaction. These conditions are appropriate to observe a fully developed glory effect in $Q(v)$, which mainly arises from the elastic scattering. Previous experiments,[30−32] involving rotationally hot

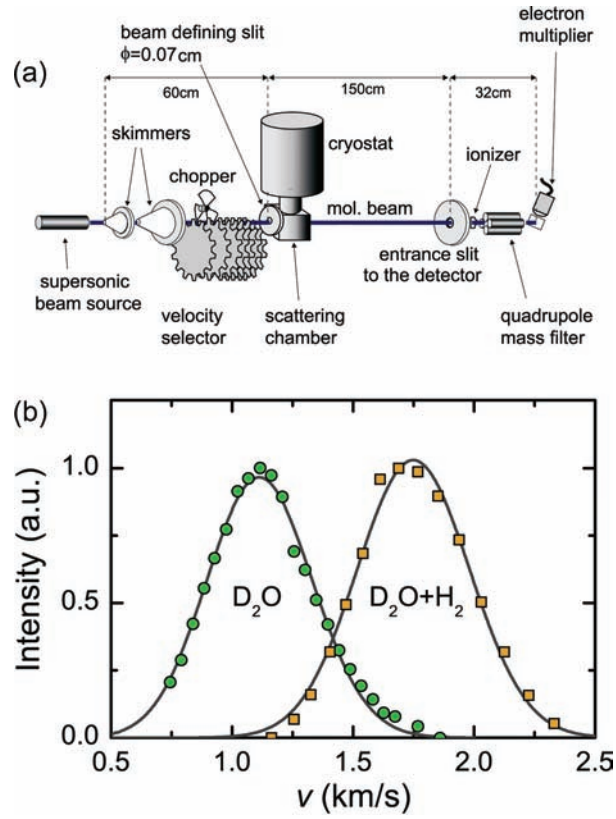

Figure 1. (a) Sketch of the experimental apparatus and (b) velocity distributions measured using in the beam source pure D_2O vapor and a D_2O-H_2 mixture in 2:1 ratio.

O_2 as a projectile scattered by the five rare gases and carried out under similar conditions, provided results that have been directly compared with the water scattering data.[27] This comparison was suggested by the very close values of the average polarizability (1.47 and 1.60 Å^3 for H_2O and O_2, respectively), a quantity found to be suitable to scale both attraction and repulsion when vdW forces are involved.[15,16] The analysis was carried out[27] using the same Morse−Spline−vdW (MSV) potential model of refs 30−32. Here we use instead a recently proposed Improved Lennard-Jones (ILJ) potential[29,33] (see below), which involves less parameters than MSV and is particularly suitable for the analysis of scattering data. The ILJ model provides an accurate representation of the interaction in a wide intermolecular distance range.[29,33] ILJ potentials have also been recently determined for the Ar−Ng complexes,[29] and those results are here exploited for further accurate comparison with the present systems. The Ar−Ng potentials must represent an upper limit of the vdW component for the homologous water−Ng and O_2-Ng systems considering, that the Ar polarizability (1.64 Å^3) is slightly larger than that of O_2 and H_2O.

The experimental apparatus used to perform the scattering experiments consists of a set of differentially pumped vacuum chambers connected by slits for MB collimation. The MB emerges through a nozzle (1 mm in diameter), from a source that can operate under nearly effusive or moderately supersonic conditions. After mechanical velocity selection, the MB crosses a scattering chamber, which can be filled with the target gas by an automated procedure. After the scattering, the online beam intensity is detected through ionization via electron bombardment followed by a quadrupole mass-spectrometric measurement. A sketch of the apparatus is shown in the upper part of Figure 1 and all the geometrical characteristics of slits and scattering chamber are given elsewhere.[34] Water MBs have been

generated by expansions of water vapor through a nozzle heated to 600 K, both to suppress cluster formation and to "heat up" the rotational motion of the water molecules. D_2O that is 100% isotopically substituted has been employed to take advantage of the fact that background noise in the mass spectrometer is much smaller at $m/e = 20$ than at $m/e = 18$. D_2O vapor has been kept in the source both pure, at a stagnation pressure of 5 mbar, and in a mixture with H_2 at a total stagnation pressure of 8 mbar, to cover a wide collision velocity range. The MB velocity analysis and selection have been obtained with the use of a slotted disk velocity selector with a high resolution (full width at half-maximum 5%). The typical velocity distributions, measured under the two operative conditions of the source, are reported in the lower part of Figure 1.

The measurement of the MB attenuation I/I_0 (were I and I_0 represent the MB intensity with and without target gas in the scattering chamber) at each selected MB velocity v, permits the determination of the integral cross section Q as a function of v, according to

$$Q(v) = -\frac{1}{NL}\log\frac{I}{I_0} \tag{1}$$

where N is the target gas density and L the effective length of the path in the scattering chamber. The scattering chamber has been kept at the liquid air temperature (~90 K) to enhance the velocity resolution of the experiments. As previously,[30−32] the absolute values of $Q(v)$ have been obtained through an internal calibration of the NL factor based on the direct measurement of the gas flow in the scattering chamber and on the absolute values of the He−Ar cross sections.[35]

The MBs of water employed contain molecules having an average rotational period of $\sim 10^{-13}$ s and should be considered rotationally "hot",[31,32,34] since the typical collision time in our experiments (i.e., the time needed to traverse a distance of $\sim 8 \times 10^{-10}$ m, corresponding to twice the glory impact parameter) is longer, ranging from 10^{-12} s (low velocities) to 3×10^{-13} s (high velocities). Therefore, water molecules rotate sufficiently fast during each collision, generating essentially elastic events, mostly driven by the isotropic interaction component.[32]

Results and Data Analysis

Measurements have been performed for all D_2O−Ng systems in a wide range of beam velocities and the integral cross sections results are plotted in Figure 2. In the semiclassical approximation the integral cross section $Q(v)$ can be written as sum of two contributions:[36,37]

$$Q(v) = \bar{Q}(v) + \Delta Q(v) \tag{2}$$

where $\Delta Q(v)$ is an oscillatory term due to the glory quantum interference effect while $\bar{Q}(v)$ is the average monotonic component of the cross section. $Q(v)$ exhibits a monotonic behavior for D_2O−He, while for all the other systems it shows the typical oscillatory pattern due to the glory effect superimposed on $\bar{Q}(v)$.

The assignment of the glory extrema order, which increases as the velocity decreases, is made as follows (see ref 37 and references therein): the observed maxima are of order 1 for D_2O−Ne, of order 2 for D_2O−Ar, of orders 2 and 3 for D_2O−Kr and D_2O−Xe; the minima are of order 1.5 for D_2O−Ar, 1.5 and 2.5 D_2O−Kr, and finally of orders 2.5 and 3.5 for D_2O−Xe.

The scattering cross section is an extremely sensitive probe of the interaction potential. In particular, the glory structure is

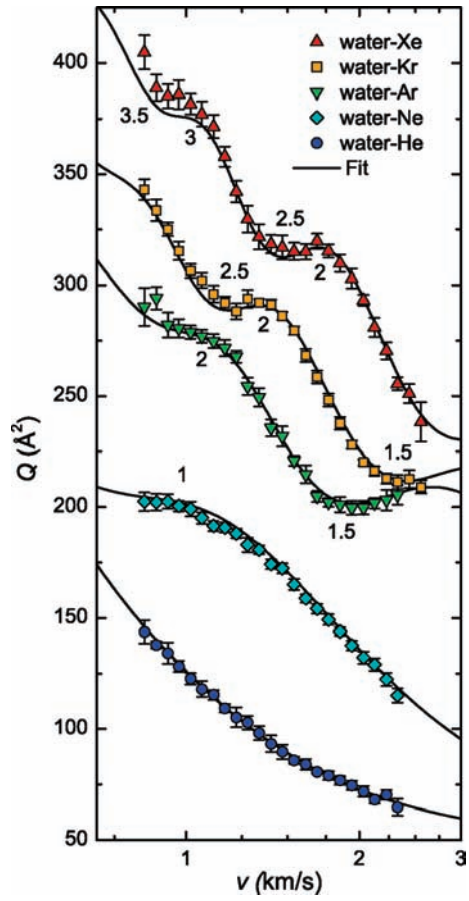

Figure 2. Cross section Q for water−Ng scattering plotted as function of the beam velocity v. Symbols are the experimental data, and lines are the fit using the ILJ potential model. The numbers represent the glory extrema order. See the text for all the details.

especially sensitive to the intermediate-range interaction (the potential well region), while $\bar{Q}(v)$ probes mainly a zone of the long-range region (see also below). Because of this, we can adopt a parametrized model potential and characterize it completely by fitting the experimental cross section. Thanks to the sufficiently high D_2O rotational temperature, a substantially isotropic interaction is expected to govern the water−Ng collisions. Therefore, a simple spherical potential model $V(r)$, where r is the intermolecular distance, can be used. The same approach has been successfully employed in the past[30−32] for the O_2 case. Previously,[27] we used a MSV potential model and details of its parametrization are given in an Appendix of ref 20. In this paper we use the ILJ model, whose functional form is the following:[29]

$$V(r) = \varepsilon\left[\frac{6}{n(r)-6}\left(\frac{r_m}{r}\right)^{n(r)} - \frac{n(r)}{n(r)-6}\left(\frac{r_m}{r}\right)^6\right] \tag{3}$$

where

$$n(r) = \beta + 4\left(\frac{r}{r_m}\right)^2 \tag{4}$$

In eq 3, the first term represents the repulsion while the second one the attraction. ε is the depth of the potential well, r_m is the equilibrium distance and β, associated with the hardness of the involved chemical species, determines the shape of the potential

TABLE 1: Experimentally Determined Well Depth ε and Equilibrium Distance r_m for the Water−Ng and Ar−Ng Systems[a]

			correlation formulas[b]			
	experimental		vdW + induction		vdW	
system	ε (meV)	r_m (Å)	ε (meV)	r_m (Å)	ε (meV)	r_m (Å)
water−He	2.75	3.45	2.94	3.40	2.57	3.42
		3.47[c]				
Ar−He	2.59	3.48			2.83	3.47
water−Ne	5.70	3.50	5.65	3.46	5.08	3.48
Ar−Ne	5.74	3.52			5.74	3.52
water−Ar	14.40	3.63	11.7	3.74	10.2	3.77
	14.42[d]	3.63[d]				
Ar−Ar	12.37	3.76			11.6	3.79
water−Kr	17.10	3.75	14.2	3.86	12.4	3.89
		3.79[e]				
Ar−Kr	14.33	3.91			14.1	3.92
water−Xe	20.20	3.93	16.1	4.04	13.9	4.07
		3.95[f]				
Ar−Xe	16.09	4.10			15.9	4.09

[a] Maximum estimated uncertainty is 3% for ε, 1% for r_m, and 2% for the εr_m product. Predictions of correlations formulas are also reported for comparison (see the text). 1 meV = 0.096485 kJ mol^{-1} and 1 Å = 0.1 nm. [b] Reference 15 and 16. [c] Reference 19b. [d] Reference 21. [e] Reference 24. [f] Reference 25.

in the region of the well. β is expected to be nearly constant for homologous systems and for the water−Ng family we use $\beta = 9$, a value typical of weak intermolecular interactions between neutral species.[29,33] Therefore, during the fitting procedure only ε and r_m have been varied, to properly reproduce extrema positions, amplitude and frequencies of $\Delta Q(v)$ and the absolute value of $\bar{Q}(v)$, the latter within the uncertainty of its calibration (3−4%).

The cross sections $Q(v)$, calculated in the center of mass frame using the JWKB method, are convoluted in the laboratory system for direct comparison with the experimental data. The convolution includes the average over the thermal motion of the target gas, the transmission function of the velocity selector, and a small correction to $Q(v)$ due to the finite angular resolution of the apparatus (the so-called "limit angle" correction, due to the uncertainty principle).[34] This is evaluated taking into account the slit dimensions and distances, the mass of the projectile, the cross section values and the probed velocity range. Figure 2 compares measured and calculated $Q(v)$, showing an excellent accord between the two. This clearly supports the validity of the isotropic model under the present experimental conditions, noting that, if the interaction anisotropy played a nonmarginal role, we would have observed a quenching of the glory amplitude.

The experimentally determined potential parameters ε and r_m are reported in the first two columns of Table 1,[38] together with previous analogous determinations, where available. As can be seen, our results agree very accurately with previous data. Note in particular the agreement with the water−Ar parameters obtained by spherical average of the accurate experimental AW2 potential of ref 21. The agreement is clearly illustrated in Figure 3, where the relevant cross sections are plotted as $Q(v)v^{2/5}$ to better separate the smooth component and emphasize amplitude and frequency of the glory pattern.

In Table 1 we also show for comparison the experimentally determined potential parameters for the Ar−Ng series.[29] As mentioned above, the comparison between the water and argon systems is naturally suggested by their similar polarizabilities, which governs vdW interactions. In this respect, it is particularly

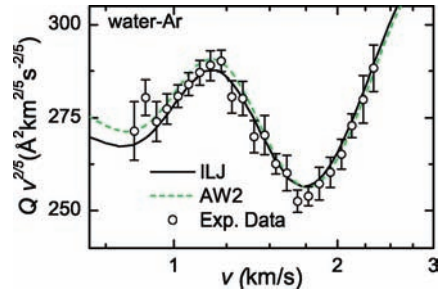

Figure 3. Measured cross section for the water−Ar system and comparison with calculations performed by using the present ILJ potential and the spherical average of the AW2 potential energy surface.[21]

instructive to examine the corresponding potential parameters derived from simple correlation formulas,[15,16] which estimate, for typical vdW systems, ε and r_m from the physical properties (in this case the polarizability) of the interacting species. These parameter estimates are also reported in Table 1 for both water−Ng and Ar−Ng. In the case of water, an additional series of figures is shown, obtained by including in the vdW model also the small induction effect, averaged over the molecular orientations, caused by water's permanent dipole (see also ref 27). What the data evidence with unequivocal clarity is that for the Ar−Ng systems the vdW correlation formulas reproduce almost exactly the experimentally determined potential parameters (well within the combined uncertainties of the model and of the experiment) while, in the case of the water complexes, agreement is only found for the two lighter Ng elements. For the heavier Ngs, discrepancies over 1 order of magnitude larger than for the argon complexes are observed. Specifically, the comparison indicates that the water−Ng adducts (Ng = Ar, Kr, Xe) are more stable by about 3−4 meV than what would be expected on the basis of the vdW + induction model, with an average equilibrium distance about 0.1 Å smaller. Note that, as Table 1 shows, according to the model, Ar and water should actually exhibit an isotropic vdW interaction with the same Ng partner, which is even more similar to what would be expected solely on the basis of the polarizability, since the presence of the small induction term in water−Ng tends to balance the smaller dispersion due to the smaller polarizability of water. Finally, it should be noted that the observed stabilization of water−Ng cannot be explained by an increase of the water dipole moment: we checked this hypothesis by calculating the interaction using the dipole value of water obtained by Saykally and co-workers[39] in the water dimer. This must in fact be considered to be a gross overestimation of the dipole in the water−Ng complexes, since the interaction in the water dimer is an order of magnitude stronger and the intermolecular distance about 1 Å shorter. Nevertheless, the resulting stabilization effect is of the order of 10^{-4} eV, much smaller than what is observed, and in fact comparable to the experimental uncertainty.

As mentioned above, the two components of $Q(v)$ in eq 1 probe the interaction potential in different ranges and it is therefore important to further validate the analysis by more quantitatively relating experimental observables and features of the interaction, which in the ILJ model essentially depend on the ε and r_m parameters.

1. The absolute value of $\bar{Q}(v)$ is affected by the long-range attraction in a specific r interval (see ref 37). Table 2 shows such intervals $[r_1, r_2]$ and other features of the long-range attraction at the distance r^* mostly probed by $\bar{Q}(v)$ (intermediate between r_1 and r_2), and also at larger r. In particular, we have chosen $x = r/r_m = 5$ where only the

TABLE 2: Smallest r_1, Largest r_2, and Mostly Probed Distance r^* by the Average Component of the Cross Section $\bar{Q}(v)$[a]

					C_6		C_{disp}		
system	r_1	r_2	r^*	$V(r^*)$	$x = 5$	$x = \infty$	this work	theory	exp
water−He					4.91	4.64	4.2	4.41[b]	4.83[c]
water−Ne	4.3	5.6	5.0	−1.02	11.1	10.5	9.5	9.70[c]	9.79[c]
					(11.6)	(10.9)		8.60[d]	
water−Ar	5.7	6.8	6.3	−0.74	34.9	32.9	30.0	30.0[d]	
					(36.8)	(34.8)		32.2[d]	
water−Kr	5.8	7.4	6.6	−0.80	50.3	47.6	43.2		
					(54.2)	(51.2)			
water−Xe	6.2	8.0	7.1	−0.80	78.8	74.4	67.7		
					(80.9)	(76.4)			

[a] Reported data are in Å. The long-range interaction $V(r^*)$ is in meV. C_6 coefficients (see text) provided by the ILJ model at different reduced values of the distance $x = r/r_m$ are in eV Å^6. The C_{disp}, extrapolated by the ILJ model, in eV Å^6, are compared with theoretical and experimental results. Data in parentheses refer to the corresponding Ar−Ng systems.[29] The estimated maximum uncertainty in the long-range coefficients is 10%. [b] Reference 18. [c] Reference 40. [d] Reference 23. [d] Reference 21.

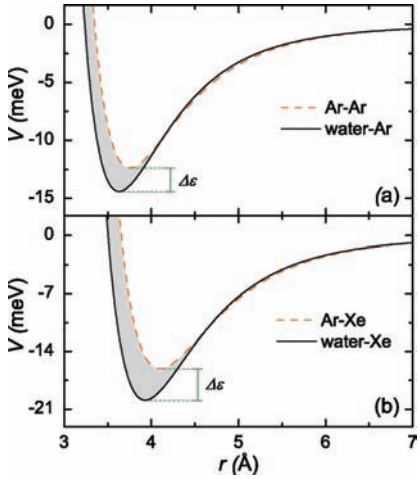

Figure 4. Comparison between the experimentally determined interaction potentials for (a) water−Ar and Ar−Ar; (b) water−Xe and Ar−Xe. The shaded areas are responsible of the glory shifts shown in Figure 6.

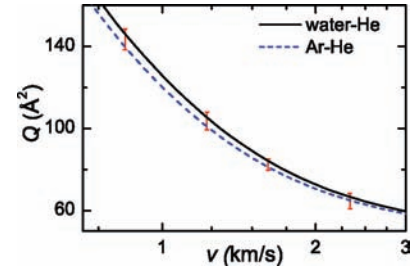

Figure 5. Comparison between the fitted cross sections of water−He and Ar−He, showing that they are essentially identical within the experimental uncertainty, indicated by vertical bars.

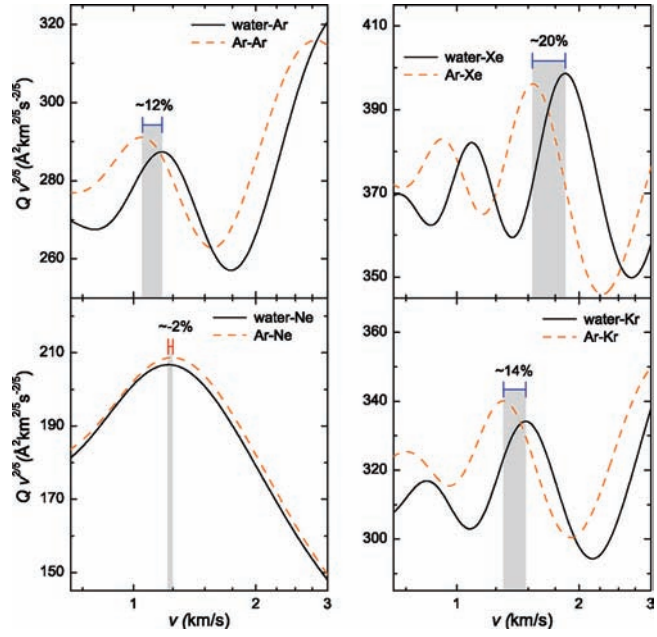

Figure 6. Comparison between the $Qv^{2/5}$ curves of the water−Ng and Ar−Ng complexes (Ng = Ne, Ar, Kr, Xe). The shaded areas evidence the shift between the glory maxima.

average dipole−dipole $C_6 = C_{disp} + C_{ind}$ coefficient contributes to the attraction, the role of the higher coefficients being negligible, and at $r \rightarrow \infty$ where the ILJ potential assumes the limiting value $C_6 = \varepsilon r_m^6$. The C_6 extrapolated from ILJ allows also an evaluation of C_{disp} by using the semiempirical relation $C_6 \simeq 1.1 C_{disp}$.[16,41] The C_{disp} values obtained from the extrapolated $C_6(x \rightarrow \infty)$, given in Table 2, appear to be in good agreement with the available experimental and theoretical values.

2. The above analysis indicates that a stabilization of the water−Ng complexes beyond the pure vdW model, increasing along the Ng series, takes hold. Figure 4 compares the experimentally determined $V(r)$, both for D_2O−Ar and Ar−Ar and for D_2O−Xe and Ar−Xe. The figure clearly shows that the corresponding potentials are indeed indistinguishable at long-range, while an additional stabilizing component emerges in the water−Ng systems at short and intermediate range, causing the deepening of the potential well, accompanied by a small but measurable reduction of the equilibrium distance (see also Table 1).
3. It is finally very meaningful to compare directly the experimental observables, namely,the scattering cross sections for the two series of complexes. The ILJ potentials for the Ar−Ng systems obtained previously[29,33] were used to reproduce the scattering cross sections observable under the present experimental conditions and these are compared with the cross sections for water−Ng in Figure 5 for Ng = He and in Figure 6 for Ng = Ne, Ar, Kr, and Xe. Figure 5 clearly shows that the interaction in Ar−He, and water−He, systems must be considered indistinguishable within the experimental uncertainty, and this confirms that water and He practically interact exclusively with the same vdW potential of Ar−He. This is also the case of Ar−Ne and water−Ne, shown in Figure 6, where the two glory maxima of order 1 appear to be coincident within the experimental resolution. Going further down along the Ng series, the picture changes dramatically, with an

TABLE 3: Computed Geometrical Parameters of the H_2O-Ng Complexes at the CCSD(T) Level with Different Basis Sets[a]

	H_2O-He		H_2O-Ne		H_2O-Ar		H_2O-Kr		H_2O-Xe	
basis	r	Φ	r	Φ	r	Φ	r	Φ	r	Φ
AVDZ	3.10	101.8	3.39	72.1	3.71	64.4	3.83	62.1	4.02	60.1
AVTZ	3.19	93.4	3.33	63.6	3.64	63.0	3.78	58.8	3.90	59.4
AVQZ	3.10	108.6	3.32	75.4	3.66	66.0	3.84	60.9	4.00	59.6
AV5Z	3.16	97.1	3.35	82.0	3.67	67.1	3.84	61.6	4.02	61.2

[a] r is in Å, Φ is in degrees.

evident and increasing shift of the glory structure toward higher velocities clearly observable for water−Ng relative to Ar−Ng (see Figure 6). Interestingly, the absolute value of the cross section remains roughly the same for corresponding systems in the two series (within the experimental uncertainty), confirming that the interaction at long-range is essentially the same for both.

We conclude that the measured glory shift, well beyond the experimental uncertainty, must arise from an additional component of the interaction, whose stabilizing effects are evident at short and intermediate range, clearly affecting the collisional phenomenology of water−Ng systems. An important suggestion as to the origin of the observed energy stabilization is given in Figure 7, where the measured glory shift between the water and Ar complexes (see Figure 6) is plotted versus the ionization potential of the Ng atoms. This shows a clear linear correlation, indicating that the scattering observable is in direct relationship with the CT capability of the Ngs. This is the most important result of the present analysis, entirely confirmed when the water−Ng scattering experiments are compared with the corresponding the O_2-Ng ones,[27] where even more pronounced glory shifts are observed.

Theoretical Calculations. The sensitivity of the experiments described above is capable of revealing an intermolecular bond stabilization energy in the water−Ng systems, relative to the Ar−Ng ones, not larger than 4 meV (about 0.4 kJ/mol). Tracing the origin of such small interaction effects is no easy task, beginning with the fact that a quantitative description of these weak intermolecular interactions requires the use of theoretical methods that describe electronic correlation accurately and large basis sets. The suggestion that the small stabilization effects evidenced by the experiments on water complexes may originate from a CT component in the interaction is a priori also difficult to prove or refute, because the CT involved may not be much larger than one or two millielectrons, which is close to the limits of arbitrariness inherent in any charge decomposition model. We have recently successfully tackled this problem[28] by performing state-of-the-art ab initio calculations on the water−Ng and Ar−Ng systems and resorting to a model-free and detailed analysis of the computed change in electron density taking place upon formation of the complexes. This is based on the study of the simple function[42]

$$\Delta q(z) = \int_{-\infty}^{\infty} dx \int_{-\infty}^{\infty} dy \int_{-\infty}^{z} dz' \, \Delta\rho(x,y,z') \qquad (5)$$

where $\Delta\rho$ is the difference between the electron density of the complex and that of the noninteracting fragments placed in exactly the same positions. By definition, $\Delta q(z)$ gives, at each point z along a chosen axis, the amount of electron charge that, upon switching on the interaction between the fragments, is displaced from the right to the left side of a plane orthogonal to the axis in z. A negative Δq thus corresponds to electron flow from left to right, while its slope is positive where charge accumulates and negative where it outflows. In this way, having fixed in space an axis of interest, which in our case joins the Ng atom with either Ar or the oxygen atom of water, $\Delta q(z)$ provides a detailed snapshot of electron charge displacement across the entire molecular region. This permits a reliable assessment of whether, where and when CT can confidently be said to take place. In this way we were able to show[28] that CT takes place in the heavier water−Ng complexes and, most important, that it essentially correlates linearly with the observed glory shifts. As an enlightening example of the kind of information that it has been possible to extract from this analysis,[28] we show in Figure 8 the Δq curve for water−Ar at their equilibrium position obtained at the CCSD/AVQZ level. The curve is negative everywhere in the molecular region, meaning that at any position along the Ar−O axis, the corresponding amount of electronic charge has been transferred from Ar toward water. Remarkably, this CT extends roughly constantly across an ample region going from about −2 Å from the oxygen atom throughout the entire region occupied by the water molecule. This means that, regardless of the exact position where a boundary is placed between the interacting fragments, roughly the same CT picture would emerge. In other words, this shows that, in this specific case, CT, although small, is essentially model-independent. To illustrate this, we show in Figure 9 the linear correlation between the measured glory shifts and three different choices of CT values. In one of them we have taken the lower limit of CT, corresponding to the maximum that the Δq curves exhibit in the region between the noble gas and water (between $z = -2$ and $z = -1$ for H_2O-Ar in Figure 8). In the second, we have taken the Δq value at the position of the hydrogen atom closer to Ng, which represents an unrealistically extreme limit of the boundary between Ng and water. And finally, we also show in the figure the CT values that result from the well-established Natural Bond Order (NBO) charge decomposition model.[8,43] Although the lines are shifted and have different slopes (corresponding, as it were, to different "units" of charge), the figure leaves little doubt as to the strict correlation between CT and the measured effects. For a more detailed discussion of the CT taking place in the water−Ng complexes, its strong anisotropy, and its relation to the experiments, please see ref. 28.

In the following we would like to focus on other, not previously discussed, aspects of the theoretical calculations performed, more directly related to the potential energy surfaces of the water−Ng and Ar−Ng interaction and the water−Ng stabilization energies.

Computational Details. All calculations have been carried out at the coupled cluster level of theory[44−46] with single, double (CCSD), and perturbatively included triple excitations (CCSD (T)) using augmented correlation consistent polarized valence basis sets up to quintuple-ζ (aug-cc-pVxZ, with x = D, T, Q, 5).[47−49] For the complexes with He, Ne, and Ar a single point energy calculation, using the sextuple-ζ aug-cc-pV6Z basis set,[50,51] has further been carried out at the geometry optimized with the aug-cc-pV5Z basis. We shall refer to these basis sets as AVxZ, with x = D, T, Q, 5, 6. For the Xe case, relativistic effects have been taken into account through the use of small-core pseudopotentials.[52] All the ab initio calculations have been carried out using the program MOLPRO.[53]

We have investigated in detail, in all cases, the basis set convergence for the determination of both the equilibrium geometry of the complexes and the corresponding interaction

TABLE 4: Computed Interaction Energy *E* (meV) of the H_2O−Ng Complexes[a]

		H_2O−He		H_2O−Ne		H_2O−Ar		H_2O−Kr		H_2O−Xe	
basis	method	*E*	BSSE	*E*	BSSE	*E*	BSSE	*E*	BSSE	*E*	BSSE
AVDZ	CCSD	5.47		10.37		20.85		26.43		27.31	
	CCSD(T)	6.19	2.41	12.61	3.877	25.28	7.96	31.92	10.07	34.01	10.31
AVTZ	CCSD	4.09		11.78		20.26		22.92		26.23	
	CCSD(T)	4.87	3.61	13.70	6.41	25.46	14.66	28.87	18.05	33.42	21.04
AVQZ	CCSD	3.67		9.76		15.77		18.15		19.85	
	CCSD(T)	4.48	4.02	11.69	7.00	21.00	16.65	24.10	19.97	26.96	23.80
AV5Z	CCSD	3.54		6.97		14.57		16.63		18.34	
	CCSD(T)	4.36	4.15	8.97	7.51	19.84	17.06	22.56	20.37	25.41	23.60
AV6Z	CCSD	3.47		6.33		13.47					
	CCSD(T)	4.29	4.20	8.31	7.63	18.65	17.21				

[a] For the CCSD(T) calculations the energy corrected for basis set superposition error (BSSE) is also reported.

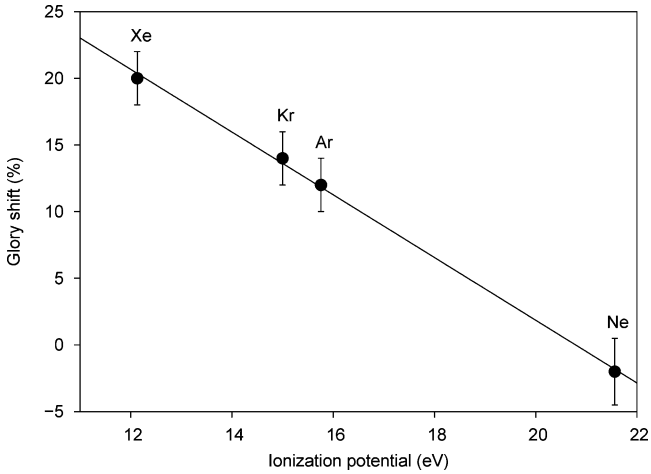

Figure 7. Correlation between the experimental shift in the cross-section glory structure of corresponding water−Ng and Ar−Ng complexes (see Figure 6) and the ionization potential of the noble gases.

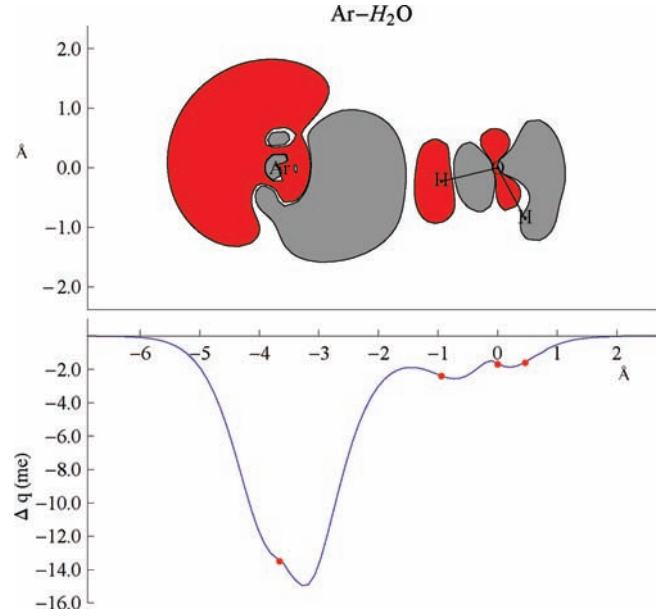

Figure 8. Upper panel: contour plot of the computed electronic density change upon formation of the H_2O−Ar complex. The red and gray areas enclose negative and positive density difference values, respectively, outside the interval $\pm 5 \times 10^{-4}$ e/bohr^3. Lower panel: $\Delta q(z)$ curve along the line connecting Ar and O. The red dots mark on the curve the z position of the nuclei.

energy. The equilibrium geometries have been determined by performing geometry optimizations at the CCSD(T) level. The water−Ng complexes are known to be planar (see, e.g., ref 54 and references therein), so the geometry optimizations have been constrained accordingly. We have found, in agreement with previous theoretical studies,[54] that the interaction with a noble gas leaves the geometry of water essentially unaffected and that the change in the interaction energy due to water geometry relaxation is negligible. For example, in H_2O−Ar we find that the O−H distances vary by less than 0.001 Å, and the H−O−H angle by less than 0.2°. For this reason, the water molecule has been kept rigid at its free equilibrium structure[55] during the geometry optimizations. The basis set superposition error (BSSE) was evaluated for all complexes using the counterpoise correction of Boys and Bernardi.[56] For H_2O−Ar an energy decomposition analysis based on the symmetry-adapted perturbation theory (SAPT)[9] has also been carried out. The SAPT calculation was done in the DCBS scheme[57] at the intramonomer CCSD level with the AVQZ basis set.

Geometry Optimizations and Interaction Energies. With frozen-geometry fragments, the geometry of the H_2O−Ng complexes may be specified by the Ng−O distance r and the angle Φ between the Ng−O axis and the symmetry axis of water, with $\Phi = 0°$ corresponding to Ng approaching from the hydrogen side. The optimized geometrical parameters and the corresponding interaction energies of the H_2O−Ng complexes, obtained with various basis sets, are reported in Table 3. The various basis sets give very similar geometries. The largest deviations are seen for the He and Ne complexes, where the interaction energy is significantly smaller than in the heavier systems and the potential energy surface flatter (see below). Table 3 shows clearly that, moving down the Ng series, the Ng atom tends to approach the water molecule along a direction progressively closer to that of an O−H bond, from the hydrogen side. In particular the angle Φ reduces from about 97 to 61° (computed at CCSD(T)/AV5Z) passing from H_2O−He to H_2O−Xe. (The angle of the O−H bond is 52.3°.)

Besides the more stable nuclear configurations, we have investigated some aspects of the potential energy surfaces. In Figure 10 we report the optimized distance Ng−O as a function of the angle Φ when the noble gas moves in the plane of the water molecule. The curves follow a very similar pattern for all the complexes, showing a minimum distance of approach at $\Phi \simeq 120°$ and a longest distance at $\Phi \simeq 40°$. The curves essentially differ for a constant shift, approximately reflecting the different Ng atomic radii. This finding already suggests that simple steric reasons cannot explain the preference of the heavier noble gases to approach the water molecule at angle that is close to the O−H direction.

Table 4 reports the water−Ng interaction energies, computed with various basis sets and the two coupled cluster levels, at

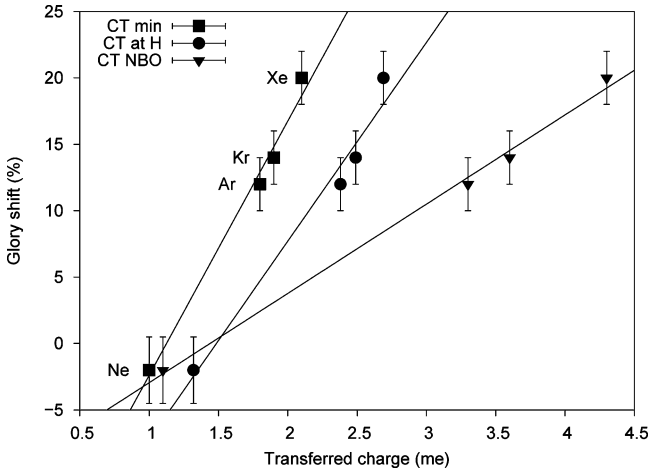

Figure 9. Correlation between the glory shift in the cross-section for corresponding water−Ng and Ar−Ng complexes (see Figure 6) and the computed CT.[28] The three series of CT values shown are the minimum $|\Delta q(z)|$ ("CT min"), the value of $|\Delta q(z)|$ at the position of the hydrogen atom closer to Ng ("CT at H"), and the NBO charge on Ng ("CT NBO").

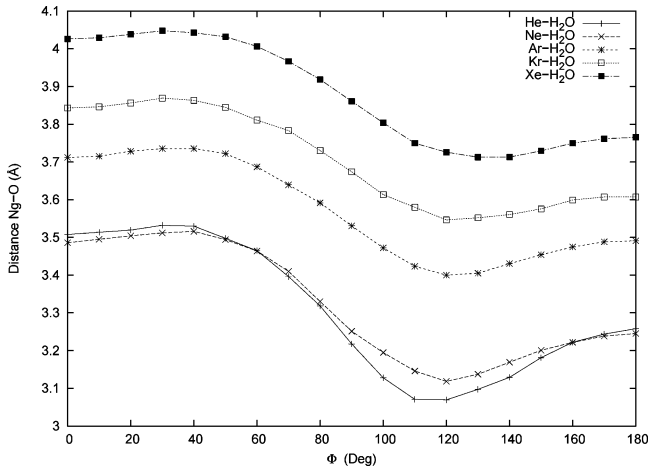

Figure 10. CCSD(T)/AV5Z optimized distance Ng−O as a function of the angle Φ.

the complex geometries optimized at the CCSD(T)/AV5Z level. The interaction energy is given as the difference between the energy of the complex and that of the isolated fragments. The table shows that obtaining accurate interaction energies for these weakly bound systems requires very large basis sets: convergence in the BSSE-corrected results (to within about 10%) is obtained only with the AVQZ basis sets. If BSSE is neglected, the computed values decrease with increasing basis set size, but when BSSE is taken into account, the trend reverses. A significant increase of the interaction energy occurs upon including triple excitations in the coupled cluster expansion, clearly indicating the large role played by electron correlation. Remarkably, this increase is found to be, for each system, nearly constant regardless of the basis set used. BSSE is unacceptably large with the smaller basis sets and in some cases, H_2O−Ne and H_2O−Ar, is still a non-negligible fraction of the binding energy calculated with the large AV5Z basis. Since BSSE invariably reduces the estimated dissociation energy, with intermediate basis sets the effect of triple excitations and BSSE tends to cancel each other out to a remarkable extent. As a comparison we performed SAPT calculations on the Ar−H_2O system. The SAPT/AVQZ calculations yield the most stable configuration for Ar−H_2O at $r = 3.70$ Å and $\Phi = 65.4°$, with an interaction energy of 18.05 meV. These results essentially agree with those obtained at the CCSD(T) level. The obtained optimized geometries and interaction energies are consistent with the most accurate calculations reported in literature (see, for example, ref 54 and references therein).

TABLE 5: Theoretical and Experimental Isotropic Well Depth ε and Equilibrium Distance r_m for the Water−Ng and Ar−Ng Systems[a]

	theoretical		experimental	
system	ε (meV)	r_m (Å)	ε (meV)	r_m (Å)
water−He	3.19	3.32	2.75	3.45
Ar−He	2.38	3.49	2.59	3.48
water−Ne	6.25	3.33	5.70	3.50
Ar−Ne	5.14	3.49	5.74	3.52
water−Ar	14.80	3.58	14.40	3.63
Ar−Ar	11.25	3.80	12.37	3.76
water−Kr	17.92	3.71	17.10	3.75
Ar−Kr	13.09	3.95	14.33	3.91
water−Xe	21.26	3.89	20.20	3.93
Ar−Xe	14.58	4.15	16.09	4.10

[a] The theoretical values for water−Ng result as the angular average of the optimized BSSE-corrected CCSD(T)/AV5Z data (see the text).

The calculated interaction energies represent an upper limit for the experimental determinations that, because of the rotationally hot water molecules, must be taken as values averaged over the relative orientations of the colliding partners. To make a more direct comparison with the experimental results, we have performed an angular averaging of both equilibrium distance and the interaction energy. The averaging was simply done by considering just the coplanar configurations, over the 19 angular points in Figure 10, using the BSSE-corrected CCSD(T)/AV5Z results. The results are shown in Table 5, where we show again for ease of comparison also the experimentally determined values of Table 1. Clearly, the averaging procedure consistently reduces the interaction energies that were obtained at the optimized geometries (see Table 4). This reduction ranges from about 1 meV for H_2O−He and H_2O−Ne to little more than 2 meV for H_2O−Kr and H_2O−Xe. In the case of the He complex the rotationally averaged equilibrium distance is 0.16 Å longer than the minimum, while it is shorter by 0.02−0.13 Å in the other cases (see Table 3). The agreement of the theoretical r_m values with the experimental determinations is excellent for all the Ar complexes, the deviations never exceeding 0.05 Å. It is similarly accurate for the heavier Ng complexes with water, and only slightly worse for the He and Ne complexes, probably due to the incomplete averaging procedure not accounting for out-of-plane configurations. Note that the averaging procedure shifts the equilibrium distance the most, and in the right direction from the absolute minimum, for the He complex. Again with the exception of the H_2O−He and H_2O−Ne complexes, the theoretical and experimental interaction energies of the water complexes agree to within 5%, the theoretical value always slightly overestimating the corresponding experimental figure. The overestimation for the He and Ne systems are 16% and 10%, respectively, but not larger than about 0.5 meV. In the case of the Ar complexes, the theoretical values always underestimate the experimental figures, with discrepancies within 10% and never larger than about 1.5 meV. All these deviations are abundantly within the possible further effects of electron correlation and basis set superposition not accounted for in the calculations (see Table 4). The computed and experimental stabilization energies of the water complexes relative to the corresponding Ar complexes, due to CT, are

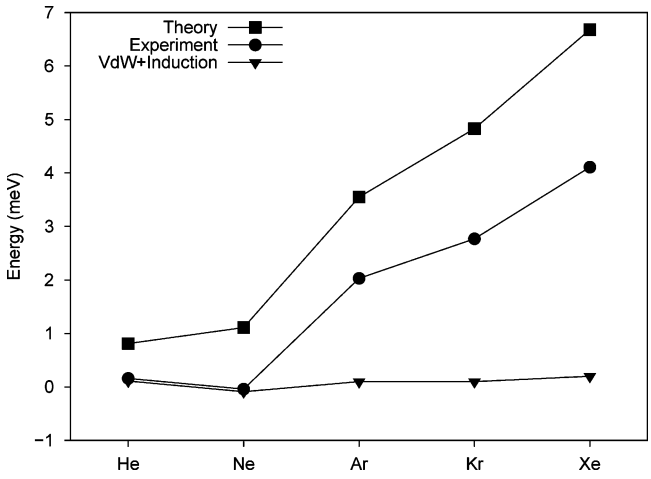

Figure 11. Computed and experimental stabilization energies of the water−Ng complexes with respect to the corresponding Ar−Ng systems. The data are from Tables 1 and 5.

directly compared in Figure 11. The theoretical curve lies systematically above the experimental one (because of the opposite sign of the error in the water and Ar complexes) but the trends match each other extremely well. The essentially vanishing energy difference curve that would be expected on the basis of the pure vdW+induction model (see Table 1) is also shown in the figure to emphasize the increasing stabilization due to CT. These results loudly confirm the analysis of the interaction potential extracted from the experimental observations and further validate the conclusion that a CT effect is measurably at work in the weakly bound water complexes.

Conclusions

In this paper we have discussed in detail a series of molecular beam scattering experiments, carried out under high angular and velocity resolution conditions, to measure quantum interference in the collisions (the "glory" effect), and aimed at directly investigating the nature of very weak intermolecular interactions involving water. By adopting a recently introduced parametrized model potential for the interaction, it is possible to fit very accurately the measured cross-section features and thus obtain accurate information on the intermolecular potential on the absolute scale. It has thus been shown in detail how well resolved modifications of the glory pattern sensitively reveal deviations from the typical van-der-Waals interaction. In particular, it has been demonstrated that while water−He can be considered a vdW aggregate, an additional component, barely noticeable in water−Ne, emerges clearly in water−Ar and becomes ever stronger in water−Kr and water−Xe. The experimental findings also demonstrate that such a component emerges at short-range, is still operative at intermediate distance, and vanishes at long-range. Recent accurate theoretical calculations have shown that an evident net CT component is indeed present in the interaction of water with the heavier noble gases. Further validating those findings, we have presented here an analysis of the angularly averaged interaction energy derived from the calculations, which matches very satisfactorily and confirms the experimental determinations.

Acknowledgment. The work has been supported by the Italian Ministero della Università e Ricerca (MIUR) through FIRB and PRIN grants. L.F.R. acknowledges the Alban Programme Scholarship.

References and Notes

(1) Müller Dethlefs, K.; Hobza, P. *Chem. Rev.* **2000**, *100*, 143.

(2) (a) Jeffrey, G. *An Introduction to Hydrogen Bonding*; Oxford University Press: New York, 1997. (b) Desiraju, G.; Steiner, T. *The Weak Hydrogen Bond in Structural Chemistry and Biology*; Oxford University Press: Oxford, U.K., 1999.

(3) *Hydrogen Bonding - New Insights*; Grabowski, S., Ed.; Springer: Dordrecht, The Netherlands, 2006.

(4) (a) Hobza, P.; Havlas, Z. *Chem. Rev.* **2000**, *100*, 4253. (b) Scheiner, S.; Kar, T. *J. Phys. Chem. A* **2002**, *106*, 1784. (c) Tatamitani, Y.; Liu, B.; Shimada, J.; Ogata, T.; Ottaviani, P.; Maris, A.; Caminati, W.; Alonso, J. *J. Am. Chem. Soc.* **2002**, *124*, 2739. (d) Alabugin, I.; Manoharan, M.; Peabody, S.; Weinhold, F. *J. Am. Chem. Soc.* **2003**, *125*, 5973. (e) Alonso, J.; Antolinez, S.; Bianco, S.; Lesarri, A.; Lopez, J.; Caminati, W. *J. Am. Chem. Soc.* **2004**, *126*, 3244. (f) Raghavendra, B.; Arunan, E. *Chem. Phys. Lett.* **2008**, *467*, 37.

(5) Kollman, P. A.; Allen, L. *Chem. Rev.* **1972**, *72*, 283.

(6) (a) Isaacs, E.; Shukla, A.; Platzman, P.; Hamann, D.; Barbiellini, B.; Tulk, C. *Phys. Rev. Lett.* **1999**, *82*, 600. (b) Ghanty, T.; Staroverov, V.; Koren, P.; Davidson, E. *J. Am. Chem. Soc.* **2000**, *122*, 1210. (c) Guo, J.-H.; Luo, Y.; Augustsson, A.; Rubensson, J.-E.; Sathe, C.; Agren, H.; Siegbahn, H.; Nordgren, J. *Phys. Rev. Lett.* **2002**, *89*, 137402. (d) Pacios, L. F.; Galvez, O.; Gomez, P. *J. Chem. Phys.* **2005**, *122*, 214307.

(7) (a) Finney, J. L. *J. Mol. Liq.* **2001**, *90*, 303. (b) Guillot, B. *J. Mol. Liq.* **2002**, *101*, 219.

(8) Reed, A.; Curtiss, L.; Weinhold, F. *Chem. Rev.* **1988**, *88*, 899.

(9) Jeziorski, B.; Moszynski, R.; Szalewicz, K. *Chem. Rev.* **1994**, *94*, 1887.

(10) van der Vaart, A.; Merz, K., Jr. *J. Chem. Phys.* **2002**, *116*, 7380.

(11) Khaliullin, R.; Bell, A. T.; Head-Gordon, M. *Chem.—Eur. J.* **2009**, *15*, 851.

(12) Sennikov, P.; Ignatov, S.; O., S. *Chem. Phys. Chem.* **2005**, *6*, 393.

(13) (a) Pfeilsticker, K.; Lotter, A.; Peters, C.; Bosch, H. *Science* **2003**, *299*, 1329. (b) Kjaergard, H.; Robinson, T.; Howard, D.; Daniel, J.; Headrick, J.; Vaida, V. *J. Phys. Chem.* **2003**, *107*, 10680.

(14) Kuma, S.; Slipchenko, M.; Kuyanov, K.; Momose, T.; Vilesov, A. *J. Phys. Chem.* **2006**, *110*, 10046.

(15) Pirani, F.; Maciel, G. S.; Cappelletti, D.; Aquilanti, V. *Int. Rev. Phys. Chem.* **2006**, *25*, 165.

(16) (a) Cambi, R.; Cappelletti, D.; Liuti, G.; Pirani, F. *J. Chem. Phys.* **1991**, *95*, 1852. (b) Cappelletti, D.; Liuti, G.; Pirani, F. *Chem. Phys. Lett.* **1991**, *183*, 297. (c) Aquilanti, V.; Cappelletti, D.; Pirani, F. *Chem. Phys.* **1996**, *209*, 299.

(17) (a) Pirani, F.; Giulivi, A.; Cappelletti, D.; Aquilanti, V. *Mol. Phys.* **2000**, *98*, 1749. (b) Klos, K.; Chalasinski, G.; Krems, R.; Buchachenko, A.; Aquilanti, V.; Pirani, F.; Cappelletti, D. *J. Chem. Phys.* **2002**, *116*, 9269. (c) Pirani, F.; Alberti, M.; Castro, A.; Moix Teixidor, M.; Cappelletti, D. *Chem. Phys. Lett.* **2004**, *394*, 37. (d) Candori, P.; Falcinelli, S.; Pirani, F.; Tarantelli, F.; Vecchiocattivi, F. *Chem. Phys. Lett.* **2007**, *436*, 322.

(18) Hodges, M.; Wheatley, R.; Harvey, A. *J. Chem. Phys.* **2002**, *116*, 1397.

(19) (a) Bickes, R. W., Jr.; Duquette, G.; van den Meijdenberg, C. J. N.; Rulis, A. M.; Scoles, G.; Smith, K. M. *J. Phys. B* **1975**, *8*, 3074. (b) Slankas, J.; Keil, M.; Kuppermann, A. *J. Chem. Phys.* **1979**, *70*, 1482. (c) Brudermann, J.; Steinbach, C.; Buck, U.; Patkowski, K.; Moszynski, R. *J. Chem. Phys.* **2002**, *117*, 11166. (d) Patkowski, K.; Korona, T.; Moszynski, R.; Jeziorski, B.; Szalewicz, K. *J. Mol. Struct. (THEOCHEM)* **2002**, *591*, 231. (e) Calderoli, G.; Cragnoni, F.; Raimondi, M. *Chem. Phys. Lett.* **2003**, *370*, 233.

(20) Cappelletti, D.; Aquilanti, V.; Cornicchi, E.; Moix-Teixidor, M.; Pirani, F. *J. Chem. Phys.* **2005**, *106*, 024302.

(21) Cohen, R. C.; Saykally, R. J. *J. Chem. Phys.* **1993**, *98*, 6007.

(22) (a) Chalasinski, G.; Szczesniak, M.; Scheiner, S. *J. Chem. Phys.* **1991**, *94*, 2807. (b) Bulski, M.; Wormer, P.; van der Avoird, A. *J. Chem. Phys.* **1991**, *94*, 8096. (c) Tao, F. M.; Klemperer, W. *J. Chem. Phys.* **1994**, *101*, 1129. (d) Burcl, R.; Chalasinski, G.; Bukowski, R.; Szczesniak, M. M. *J. Chem. Phys.* **1995**, *103*, 1498.

(23) Hodges, M.; Wheatley, R.; Harvey, A. *J. Chem. Phys.* **2002**, *117*, 7169.

(24) van Wijngaarden, J.; Jäger, W. *Mol. Phys.* **2000**, *98*, 1575.

(25) Wen, Q.; Jäger, W. *J. Phys. Chem. A* **2006**, *110*, 7560.

(26) Maitland, G. C.; Rigby, M.; Smith, E. B.; Wakeham, W. A. *Intermolecular Forces: Their origin and Determination*; Clarendon Press: Oxford, U.K., 1987

(27) Aquilanti, V.; Cornicchi, E.; Moix Teixidor, M.; Saendig, N.; Pirani, F.; Cappelletti, D. *Angew. Chem. Int. Ed.* **2005**, *44*, 2356.

(28) Belpassi, L.; Tarantelli, F.; Pirani, F.; Candori, P.; Cappelletti, D. *Phys. Chem. Chem. Phys.,* in press.

(29) Pirani, F.; Brizi, S.; Roncaratti, L. F.; Casavecchia, P.; Cappelletti, D.; Vecchiocattivi, F. *Phys. Chem. Chem. Phys.* **2008**, *10*, 5489.

(30) Luzzatti, E.; Pirani, F.; Vecchiocattivi, F. *Mol. Phys.* **1977**, *34*, 1279.

(31) (a) Pirani, F.; Vecchiocattivi, F. *Chem. Phys.* **1981**, *59*, 387. (b) Pirani, F.; Vecchiocattivi, F.; van den Biesen, J. J. H.; van den Meijdenberg, C. J. N. *J. Chem. Phys.* **1981**, *75*, 1042.

(32) Aquilanti, V.; Ascenzi, D.; Cappelletti, D.; de Castro, M.; Pirani, F. *J. Chem. Phys.* **1998**, *109*, 3898.

(33) Candori, P.; Cappelletti, D.; Falcinelli, S.; Pirani, F.; Roncaratti, L. F.; Tarantelli, F.; Vecchiocattivi, F. *Phys. Scr.* **2008**, *78*, 038102.

(34) Cappelletti, D.; Bartolomei, M.; Pirani, F.; Aquilanti, V. *J. Phys. Chem. A* **2002**, *106*, 10764.

(35) Nenner, T.; Tien, H.; Fenn, J. *J. Chem. Phys.* **1975**, *63*, 5439.

(36) Bernstein, R. B. *Adv. Chem. Phys.* **1966**, *10*, 75.

(37) Pirani, F.; Vecchiocattivi, F. *Mol. Phys.* **1982**, *45*, 1003.

(38) Although the present analysis has been carried out with a different potential model, the ε and r_m parameters here obtained for the water−Ng systems agree with those presented in ref 27 except for a small variation of ε for the water−Xe system. Note further that the use of D_2O instead of H_2O involves a 0.05 Å shift of the molecular center-of-mass away from the oxygen atom. However, the spherical average carried out over the potential energy surface yields essentially identical results for the two isotopes.

(39) Liu, K.; Brown, M.; Saykally, R. *J. Phys. Chem. A* **1997**, *101*, 8995.

(40) Olney, T. N.; Cann, N. M.; Cooper, G.; Brion, C. E. *Chem. Phys.* **1997**, *223*, 59.

(41) Buckingham, A. D. *Adv. Chem. Phys.* **1967**, *12*, 107.

(42) Belpassi, L.; Infante, I.; Tarantelli, F.; Visscher, L. *J. Am. Chem. Soc.* **2008**, *130*, 1048.

(43) Glendening, E. D.; Badenhoop, J. K.; Reed, A. E.; Carpenter, J. E.; Bohmann, J. A.; Morales, C. M.; Weinhold, F. NBO 5.G; Theoretical Chemistry Institute, University of Wisconsin: Madison, WI, 2001; http://www.chem.wisc.edu/~nbo5.

(44) Raghavachari, K.; Trucks, G. W.; Pople, J. A.; Head-Gordon, M. *Chem. Phys. Lett.* **1989**, *157*, 479.

(45) Hampel, C.; Peterson, K. A.; Werner, H.-J. *Chem. Phys. Lett.* **1992**, *190*, 1.

(46) Deegan, M. J. O.; Knowles, P. J. *Chem. Phys. Lett.* **1994**, *227*, 321.

(47) Dunning, T. H. *J. Chem. Phys.* **1989**, *90*, 1007.

(48) Woon, D. E.; Dunning, T. H. *J. Chem. Phys.* **1994**, *100*, 2975.

(49) Woon, D. E.; Dunning, T. H. *J. Chem. Phys.* **1993**, *98*, 1358.

(50) Wilson, A. K.; van Mourik, T.; Dunning, T. H. *J. Mol. Struct. (THEOCHEM)* **1996**, *388*, 339.

(51) Peterson, K. A.; Woon, D. E. http://gnode2.pnl.gov.

(52) Peterson, K. A.; Figgen, D.; Goll, E.; Stoll, H.; Dolg, M. *J. Chem. Phys.* **2003**, *119*, 11113.

(53) Werner, H.-J.; Knowles, P. J.; Lindh, R.; Manby, F. R.; Schütz, M. Molpro version 2006.1, a package of ab initio programs, see http://www.molpro.net.

(54) Makarewicz, J. *J. Chem. Phys.* **2008**, *129*, 184310.

(55) Mas, E. M.; Szalewicz, K. *J. Chem. Phys.* **1996**, *104*, 7606.

(56) Boys, S. F.; Bernardi, F. *Mol. Phys.* **1970**, *19*, 553.

(57) Bukowski, R.; Cencek, W.; Jankowski, J.; Jeziorska, M.; Jeziorski, B.; Kucharski, S. A.; Lotrich, V. F.; Misquitta, A. J.; Moszyński, R.; Patkowski, K.; Podeszwa, R.; Rybak, S.; Szalewicz, K.; Williams, H. L.; Wheatley, R. J.; Wormer, P. E. S.; Zuchowski, P. S. SAPT2008: An Ab Initio Program for Many-Body Symmetry-Adapted Perturbation Theory Calculations of Intermolecular Interaction Energies. Sequential and parallel versions. User's Guide, see http://www.physics.udel.edu/szalewic/SAPT/SAPT.html.

JP905584P